

Nonreciprocity of a six-wave mixing light droplet by a moving electromagnetically induced grating

Yiqi Zhang, Zhenkun Wu, Huaibin Zheng, Zhiguo Wang, Yunzhe Zhang, Hao Tian and Yanpeng Zhang

Key Laboratory for Physical Electronics, Devices of the Ministry of Education & Shaanxi Key Lab of Information Photonic Technique, Xi'an Jiaotong University, Xi'an 710049, People's Republic of China

E-mail: ypzhang@mail.xjtu.edu.cn

Received 2 December 2013, revised 3 January 2014

Accepted for publication 19 January 2014

Published 17 March 2014

Abstract

For the first time, we investigate the nonreciprocal generation of six-wave mixing (SWM) in an inverted-Y type four-level system with spatially uniform distribution of atoms. The nonreciprocity results from a moving electromagnetically induced grating (EIG) which is formed by two coupling beams with different frequencies. We demonstrate that the nonreciprocity can be controlled by the frequencies of the coupling fields and the powers of the dressing beams. As the distribution of atoms is uniform, the atomic density cannot affect the nonreciprocity, but it will affect the formation of the photonic band gap structure of the moving EIG. This research can be used to make optical diodes or optical isolators, because the moving EIG, the speed of which is related to the frequency difference of the two coupling beams, can break time-reversal symmetry. We also demonstrate that the nonreciprocal SWM can form a nonreciprocal light droplet when it propagates in atomic vapors with third- and fifth-order nonlinear susceptibilities.

Keywords: multi-wave mixing, moving electromagnetically induced grating, nonreciprocity

(Some figures may appear in colour only in the online journal)

1. Introduction

Optical reciprocity is a ubiquitous phenomenon, which indicates that the source and detection positions can be exchanged without changing the optical properties. For a long time, scientists have made a great deal of effort and invented several methods to obtain the optical nonreciprocity, which has potential applications in producing optical diodes. Such efforts have been reported in parity-time symmetric media [1, 2], media with magneto-optical effects [3] or acousto-optical effects [4], non-symmetric photonic crystals [5], etc. However, the efficiency of the nonreciprocity output is quite low.

Very recently, it has been found that a moving photonic crystal [6] can lead to optical nonreciprocal transmission, which had been rather difficult to achieve ever before. This

elaborate result is obtained in an electromagnetically induced transparency (EIT) atomic medium with spatially uniform distribution of atoms, in which a standing wave in motion is formed by two laser beams with different frequencies through mutual interference. The standing wave is also called an electromagnetically induced grating (EIG) [7, 8], which possesses photonic band gap (PBG) structure. As the EIG is moving, a probe laser beam incident into the EIG along or opposite to the moving direction will be reflected in a different frequency range because of the Doppler effect; that is to say, the PBG is different for the same probe, which leads to nonreciprocal transmission. It is worth mentioning that Bragg mirrors in motion formed by periodically distributed atoms can also lead to nonreciprocal transmission [9].

As EIT and EIT media have many advantages, such as absorption reduction, nonlinearity enhancement, easy control

and integration on chips, to name a few, research topics related to EIT have attracted a lot of attention. In recent decades, we have investigated and observed the coexistence of four-wave mixing (FWM) and six-wave mixing (SWM) [10], enhancement and suppression of nonlinear susceptibilities [11], multi-wave mixing (MWM) band gap solitons [12] and vortex solitons [13], and so on. In addition, we have also devoted much effort into PBG investigations in EIT atomic vapors.

In this paper, we investigate the nonreciprocal generation of SWM in an inverted-Y type energy system. A moving EIG is fabricated by interference of two coupling beams with different frequencies. When probes are incident onto the moving EIG from different sides, the PBGs for probes on different sides will be different. Thus, different reflections of the probe beam due to the PBGs will be obtained and the observed SWM will be nonreciprocal. In addition, we also find that the nonreciprocal SWM can form nonreciprocal light droplets in atomic vapors with third- and fifth-order nonlinear susceptibilities.

2. Basic theory

We consider an inverted-Y type four-level atomic system composed of the $5S_{1/2}(F=3)(|0\rangle)$, $5S_{1/2}(F=2)(|1\rangle)$, $5P_{3/2}(2)(|2\rangle)$, and $5D_{5/2}(3)(|3\rangle)$ levels of ^{85}Rb , as shown in figure 1(a). Coupling laser beams E_3 and E'_3 connect the transition $|0\rangle \rightarrow |2\rangle$, dressed laser beam E_2 connects $|2\rangle \rightarrow |3\rangle$, and the probe laser beam E_1 connects $|1\rangle \rightarrow |2\rangle$. The beams will generate SWM signals, as depicted in figure 1(b). The coupling field can be written as $\mathbf{E}_c = \hat{y}[E_3 \cos(\omega_3 t - k_3 x) + E'_3 \cos(\omega'_3 t + k'_3 x)]$, which will form a moving standing wave, i.e. a moving EIG. The Rabi frequency of the coupling field is $G_3 = \mu E_c / \hbar$, so that we have

$$|G_3|^2 = \frac{\mu^2}{\hbar^2} [E_3^2 + E_3'^2 + 2E_3 E_3' \cos(\delta t + 2k_c x)], \quad (1)$$

in which the frequency detuning $\delta = \omega'_3 - \omega_3$ and $k_c = (\omega'_3 + \omega_3)/2c$ with c the speed of light in vacuum. The moving speed of the EIG is $v = -\delta/2k_c$. If we fix ω_3 and change ω'_3 to detune the moving direction and speed, we can obtain the effective period of the moving EIG, as shown in figure 1(b),

$$D = \pi \left/ \left(k_3 + \frac{\delta}{2c} \right) \right.,$$

from which we can see that D is larger for $\delta < 0$ than for $\delta > 0$. Here, we would like to emphasize that the effective period D results from the Doppler effect. If we take the moving EIG as a reference, the period of the EIG is fixed. In other words, for the same probe incidence, D is different when the moving velocity of the EIG is different. This would lead to different reflectivity and transmissivity.

According to the energy system and Liouville pathways [14], the first-order density matrix element can be written as

$$\rho_{21}^{(1)} = \frac{iG_1}{d_{21} + |G_3|^2/d_{01} + |G_2|^2/d_{31}}.$$

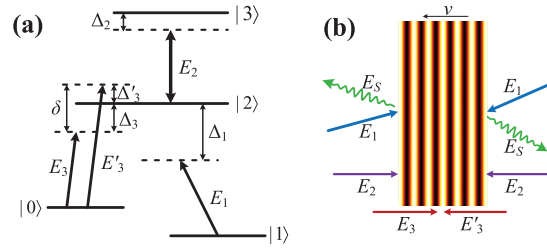


Figure 1. (a) Inverted-Y type energy system. (b) Schematic of a moving EIG formed by two coupling beams E_3 and E'_3 . Together with two dressed beams E_2 and probe E_1 , an SWM signal E_S will be generated according to the phase-matching condition $\mathbf{k}_S = \mathbf{k}_1 + \mathbf{k}_2 - \mathbf{k}_2 - \mathbf{k}_3 + \mathbf{k}'_3$ (left) or $\mathbf{k}_S = \mathbf{k}_1 + \mathbf{k}_2 - \mathbf{k}_2 + \mathbf{k}_3 - \mathbf{k}'_3$ (right).

The third- and fifth-order density matrix elements are

$$\rho_{21}^{(3)} = \frac{-iG_1|G_2|^2}{(d_{21} + |G_3|^2/d_{01} + |G_2|^2/d_{31})^2 d_{31}},$$

$$\rho_{21}^{(5)} = \frac{iG_1|G_2|^4}{(d_{21} + |G_3|^2/d_{01} + |G_2|^2/d_{31})^3 (d_{31})^2},$$

in which $d_{21} = \Gamma_{21} + i\Delta_1$, $d_{01} = \Gamma_{01} + i\Delta_1 - i\Delta_3$, $d_{31} = \Gamma_{31} + i\Delta_1 + i\Delta_2$, $\Delta_1 = \Omega_{10} - \omega_1$ and $\Delta_2 = \Omega_{20} - \omega_3$ are the detunings of the probe and coupling fields, and Γ_{10} and Γ_{30} denote the population decay rates between corresponding energy levels. Here, we should note that ω'_3 and ω_3 are different but the difference is really small, so the difference between Δ_3 and Δ'_3 is also small. In addition, the double-photon detuning $\Delta_1 - \Delta_3$ is insensitive to the single-photon detuning Δ_3 [6]; as a result, it is reasonable to just use Δ_3 to make an approximation in d_{01} . Considering that the atom velocities can only affect the single-photon detuning but not the double-photon detuning, the moving property also conserves the thermal motion.

To be frank, the moving EIG here cannot be totally viewed as a truly moving grating fabricated on a solid material, the PBG structure of which is fixed. As shown in equation (1), the period of the moving EIG changes with δ , so that the PBG structure is also different for different δ .

According to the relation $\epsilon_0 \chi E = N \mu \rho$, in which μ is the transition electric dipole moment and N is the atom density, we have the formula of the total susceptibility,

$$\chi = \frac{iN\mu^2}{\epsilon_0 \hbar} \left[\frac{1}{d_{21} + |G_3|^2/d_{01} + |G_2|^2/d_{31}} - \frac{|G_2|^2}{(d_{21} + |G_3|^2/d_{01} + |G_2|^2/d_{31})^2 d_{31}} + \frac{|G_2|^4}{(d_{21} + |G_3|^2/d_{01} + |G_2|^2/d_{31})^3 (d_{31})^2} \right]. \quad (2)$$

3. Numerical results and discussion

According to equation (1), the susceptibility given in equation (2) is moving and periodic. By using the plane-wave expansion method [15], we can obtain the PBG structures versus δ and Δ_1 as shown in figure 2(a), which is for the left probe as illustrated in figure 1(b). The corresponding

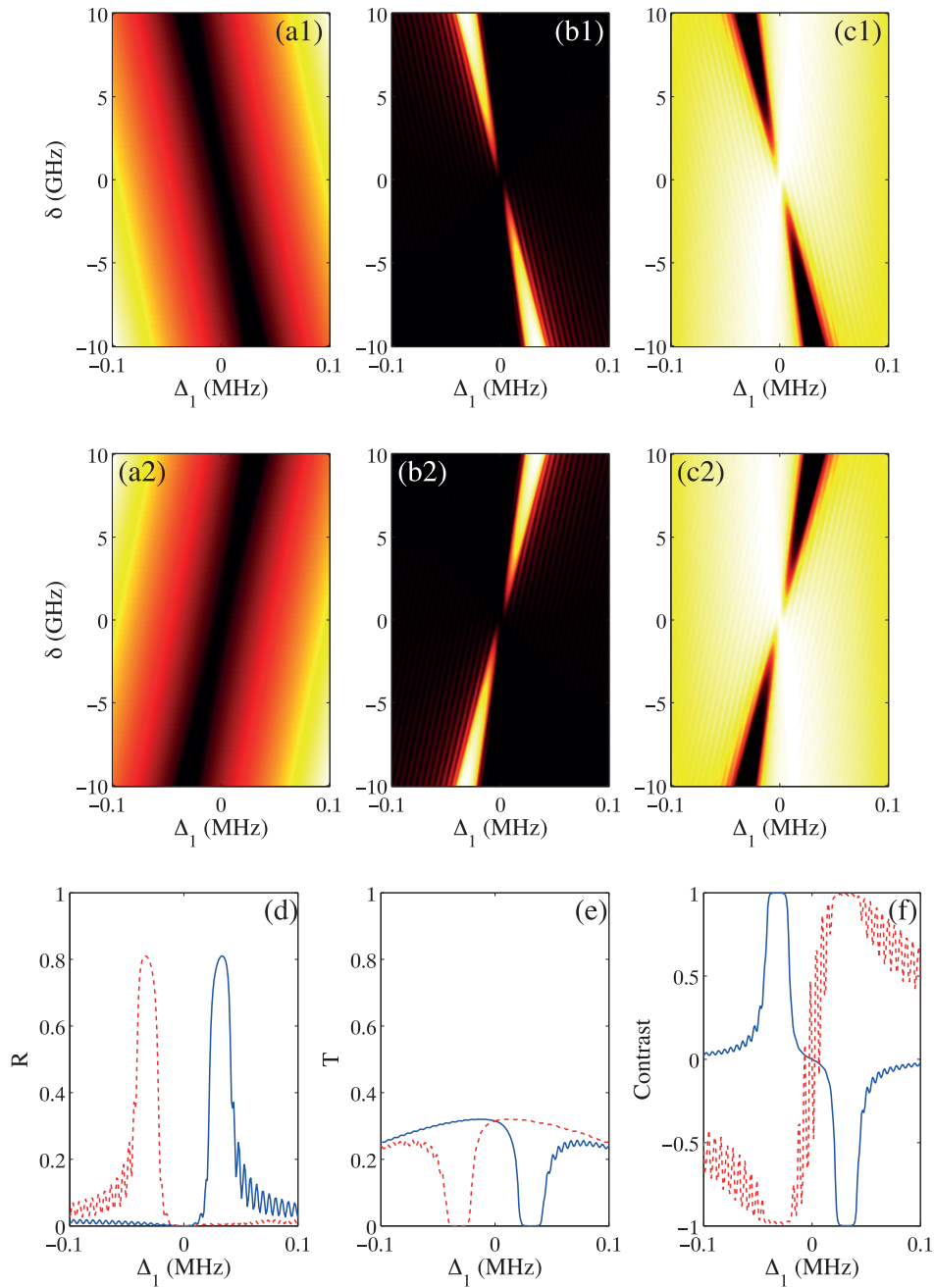


Figure 2. (a) The PBG structure. The dark regions are the PBG. (b) The reflectivity. The brightest regions mean that the reflection is the largest. (c) The transmissivity. The darkest regions mean that the transmission is the smallest. The panels in (a)–(c) are versus δ and Δ_1 . (d) The reflectivities for $\delta = 10$ GHz (solid curve) and -10 GHz (dashed curve), respectively. (e) The same as (d) but for transmissivities. (f) The contrast of the reflectivity (dashed curve) and transmissivity (solid curve) with $\delta = -10$ GHz, respectively. The parameters are $\Gamma_{21} = 10$ MHz, $\Gamma_{01} = 1$ kHz, $\Gamma_{31} = 15$ MHz, $G_3 = 35$ MHz, $G'_3 = 10$ MHz, $G_2 = 10$ MHz, $N = 10^{12}$ cm $^{-3}$ and $\lambda_1 = \lambda_3 = 770.778$ nm.

reflectivities and transmissivities are shown in figures 2(b1) and (c1), respectively. For the right probe, the PBG structure, reflectivity, and transmissivity are shown in figures 2(a2), (b2), and (c2), respectively. It is clear to see that the PBG structure is located in different places for left and right incident probes when δ is fixed. Thus, the reflectivity and transmissivity are different for the same probe when the EIG is moving along a different direction. As a result, reflectivity nonreciprocity as well as transmissivity nonreciprocity is achieved.

To make a comparison, we display the reflectivities and transmissivities with $\delta = 10$ GHz (solid curve) and -10 GHz (dashed curve) in figures 2(d) and (e), respectively. It is worth noting that the $\delta = 10$ GHz and -10 GHz cases are analogous to the results corresponding to left and right incident probes, respectively. The results also demonstrate that the reflectivity and transmissivity are nonreciprocal.

As SWM can be viewed as a Bragg reflection of the PBG from the probe (figure 1(b)), and the PBG range is different

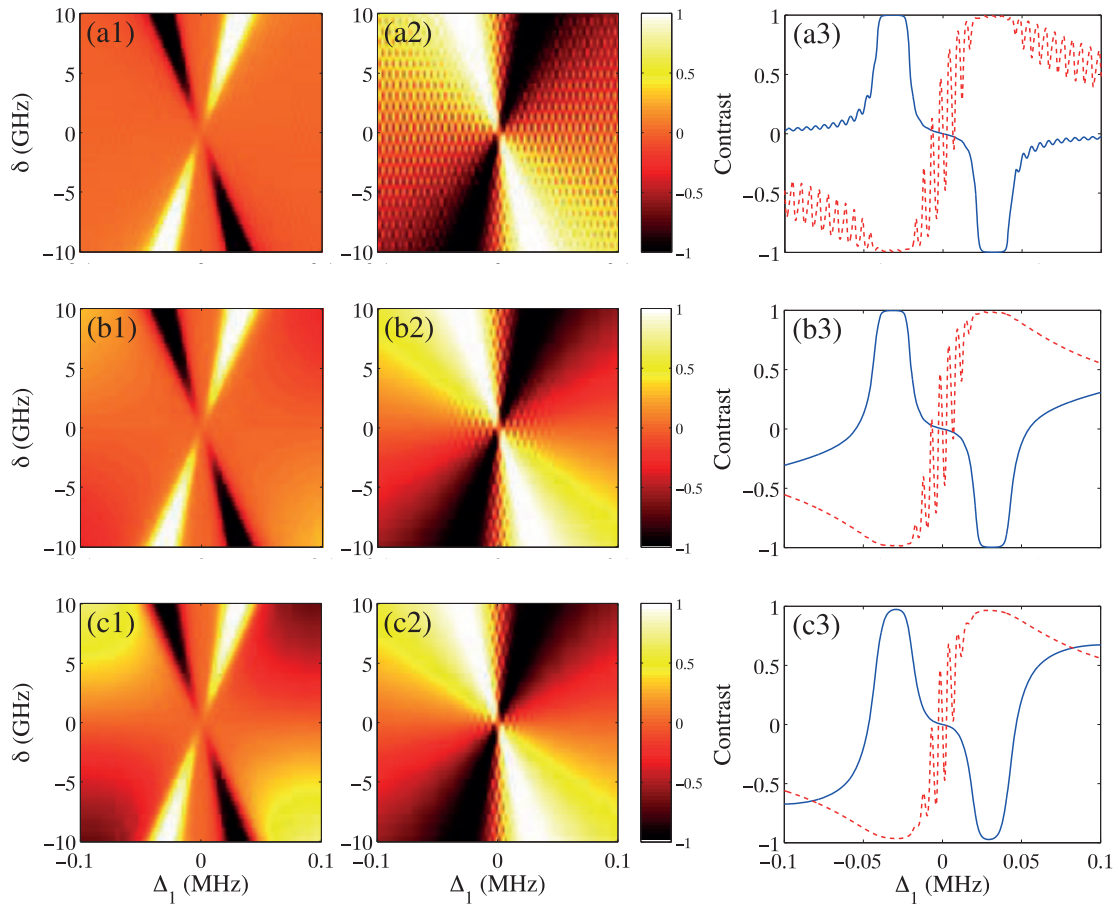


Figure 3. The contrast of the transmissivity (left panels) and reflectivity (middle panels). The right panels are configured in the same way as figure 2(f). $G_2 = 0, 100$ MHz, and 200 MHz for (a), (b), and (c), respectively. The other parameters are the same as in figure 2.

for left and right incident probes according to figure 2, the generated SWM is completely nonreciprocal. It is also clear to see from figure 2 that for the same incident probe, if the moving velocity of the EIG changes, the PBG range also changes, which indicates that the frequency of the observed SWM will be different. In other words, the nonreciprocity of the SWM can be controlled by detuning the frequencies of the coupling beams.

In figure 2(f), we show the contrast in the reflection and the transmission according to $\eta_R = (R_l - R_r)/(R_l + R_r)$ and $\eta_T = (T_l - T_r)/(T_l + T_r)$. The contrast can be viewed as a base for making optical diodes or isolators. For $\eta_R = 1$ (or $\eta_T = -1$) and $\eta_R = -1$ (or $\eta_T = 1$), the reflection and transmission of the PBG are the largest and smallest, respectively. Therefore, the requirement of unidirectional continuity of diode operation is achieved. As indicated in previous literature [6, 9], the core reason for the reciprocity is the breaking of time-reversal symmetry due to the product δt in equation (1).

In addition to the coupling frequency detuning, the power of the dressed beams E_2 can also affect the nonreciprocity. When G_2 is larger, the PBG of the moving EIG becomes less good than before, and the contrasts η_R and η_T of the reflection and transmission will be somewhat affected. In figures 3(a)–(c), we exhibit the η_R and η_T versus δ and Δ_1 for several selected powers of E_2 . Similarly to figure 2(f), we also

exhibit η_R and η_T with $\delta = -10$ MHz in figures 3(a3)–(c3), from which we can see that, with the power of E_2 increasing, the regions $\eta_R \sim 1$ and $\eta_T \sim 1$ shrink, which means that the efficiency of the nonreciprocity becomes poor. On the other hand, the oscillations appearing in η_R and η_T gradually become smaller with increase of G_2 for the same δ , which can be seen in the panels in figure 3.

As the third- and fifth-order susceptibilities are considered simultaneously in equation (2), the nonlinearity of the atomic vapor is cubic–quintic type, which will support formation of the so-called ‘light droplet’ when a beam propagates in such a medium [16, 17] according to the nonlinear Schrödinger equation

$$2ik \frac{\partial E}{\partial z} + \left(\frac{\partial^2}{\partial x^2} + \frac{\partial^2}{\partial y^2} \right) E = -k^2 \chi E.$$

Thus, the generated nonreciprocal SWM signals will form light droplet-like structures. Considering that the SWM signals may be generated from both sides of the EIG and the nonreciprocity of the SWM signals, the light droplets formed from SWM signals are also nonreciprocal. However, we should emphasize that the light droplets look the same no matter which SWM signals they are from. The main difference among the light droplets is the frequency (the same as the SWM signals).

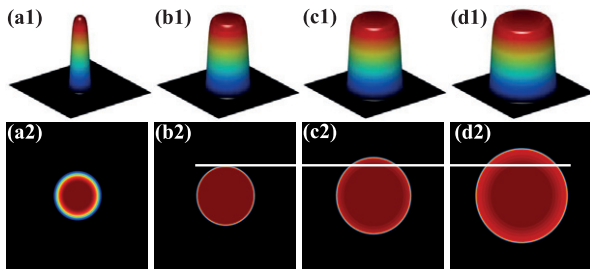


Figure 4. Formation of a light droplet from the nonreciprocal SWM resulting from the left incident probe. Top panels: intensities at different propagation distances. Bottom panels: the same as the top panels but top views. The input is a super-Gaussian beam $E = A \exp[-(r/r_0)^{10}]$ with $A = 25$ and $r_0 = 0.8$ mm. The numerical box is $2.5 \text{ mm} \times 2.5 \text{ mm}$. The propagation distances in (a)–(d) are 0, 1 cm, 4 cm, and 5 cm, respectively.

Therefore, we only show the formation of light droplets without discussing which side they are from.

In figure 4, the formation of a light droplet from two-dimensional SWM is displayed. It is clear to see that the incident nonreciprocal SWM with a Gaussian-like profile as shown in figure 4(a) will evolve into a structure with a flat top and sharply decaying edge gradually, as shown in figures 4(b1)–(d1). The flat top and sharply decaying edge of the structure are analogous to the force equilibrium and surface tension of a liquid droplet. From figures 4(b2)–(d2), we can find that there is a core in the flat top. Interestingly, the core remains almost the same upon propagation, as indicated by the white solid line.

4. Conclusion

In summary, we have demonstrated the generation of nonreciprocal SWM in a spatially uniform distributed atom medium through a moving EIG, which is the result of interference between two coupling fields with different frequencies. The nonreciprocity possesses high efficiency and can be used to produce optical diodes. In addition, we also demonstrate that the nonreciprocal SWM can form a nonreciprocal light droplet in systems with third- and fifth-order nonlinear susceptibilities.

Acknowledgments

This work was supported by the 973 Program (2012CB921804), the National Natural Science Foundation of China

(No. 61308015, No. 61078002, No. 61078020, No. 11104214, No. 61108017, No. 11104216, No. 61205112), the Specialized Research Fund for the Doctoral Program of Higher Education of China (No. 20110201110006, No. 20110201120005, No. 20100201120031), the Fundamental Research Funds for the Central Universities (No. 2012jdhz05, No. 2011jdhz07, No. xjj2011083, No. xjj2011084, No. xjj2012080, No. xjj2013089), and China Postdoctoral Science Foundation (No. 2012M521773).

References

- [1] Rüter C E, Makris K G, El-Ganainy R, Christodoulides D N, Segev M and Kip D 2010 *Nature Phys.* **6** 192
- [2] Feng L, Xu Y-L, Fegadolli W S, Lu M-H, Oliveira J E B, Almeida V R, Chen Y-F and Scherer A 2013 *Nature Mater.* **12** 108
- [3] Zaman T R, Guo X and Ram R J 2007 *Appl. Phys. Lett.* **90** 023514
- [4] Kang M S, Butsch A and Russell P St J 2011 *Nature Photon.* **5** 549
- [5] Serebryannikov A E 2009 *Phys. Rev. B* **80** 155117
- [6] Wang D-W, Zhou H-T, Guo M-J, Zhang J-X, Evers J and Zhu S-Y 2013 *Phys. Rev. Lett.* **110** 093901
- [7] Zhang Y P, Wang Z G, Nie Z Q, Li C B, Chen H X, Lu K Q and Xiao M 2011 *Phys. Rev. Lett.* **106** 093904
- [8] Zhang Y P, Yuan C Z, Zhang Y Q, Zheng H B, Chen H X, Li C B, Wang Z G and Xiao M 2013 *Laser Phys. Lett.* **10** 055406
- [9] Horsley S A R, Wu J-H, Artoni M and La Rocca G C 2013 *Phys. Rev. Lett.* **110** 223602
- [10] Zhang Z Y, Xue X X, Li C B, Cheng S J, Han L, Chen H X, Zheng H B and Zhang Y P 2012 *Opt. Commun.* **285** 3627
- [11] Wang Z G, Zhang Y P, Chen H X, Wu Z K, Fu Y X and Zheng H B 2011 *Phys. Rev. A* **84** 013804
- [12] Zhang Y P, Wang Z G, Zheng H B, Yuan C Z, Li C B, Lu K Q and Xiao M 2010 *Phys. Rev. A* **82** 053837
- [13] Zhang Y P, Nie Z Q, Zhao Y, Li C B, Wang R M, Si J H and Xiao M 2010 *Opt. Express* **18** 10963
- [14] Zhang Y P and Xiao M 2009 *Multi-Wave Mixing Processes: From Ultrafast Polarization Beats to Electromagnetically Induced Transparency* (Berlin: Springer)
- [15] Wu J-H, Artoni M and La Rocca G C 2008 *J. Opt. Soc. Am. B* **25** 1840
- [16] Michinel H, Paz-Alonso M J and Pérez-García V M 2006 *Phys. Rev. Lett.* **96** 023903
- [17] Zhang Y Q, Wu Z K, Yuan C Z, Yao X, Lu K Q, Belić M and Zhang Y P 2012 *Opt. Lett.* **37** 4507